Novel Luminescent Polynuclear Gold(I) Phosphine Complexes. Synthesis, Spectroscopy, and *X*-Ray Crystal Structure of $[Au_3(dmmp)_2]^{3+}$ [dmmp = bis(dimethylphosphinomethyl)methylphosphine]†

Vivian Wing-Wah Yam*
Department of Applied Science, City Polytechnic of Hong Kong, Tat Chee Avenue, Kowloon, Hong Kong
Ting-Fong Lai and Chi-Ming Che
Department of Chemistry, University of Hong Kong, Pokfulam Road, Hong Kong

Reaction of $K[AuCl_4]$ with bis(dimethylphosphinomethyl)methylphosphine (dmmp) in the presence of thiodiglycol (2,2′-thiodiethanol) in methanol yielded $[Au_3(dmmp)_2]^{3+}$, which was isolated as its perchlorate salt. The *X*-ray crystal structure of $[Au_3(dmmp)_2][ClO_4]_3$ has been determined: monoclinic, space group $P2_1/n$, a = 12.880(3), b = 14.210(1), c = 21.208(2) Å, β = 106.25(1)°, Z = 4, R = 0.047 for 2 927 observed Mo-K_α data. The Au–Au–Au bond angle of 136.26(4)° is greatly distorted from rectilinear geometry, with intramolecular Au • • • Au distances of 2.981(1) and 2.962(1) Å. Excitation of a degassed acetonitrile solution of $[Au_3(dmmp)_2]^{3+}$ at 300—370 nm resulted in dual phosphorescence (λ = 467 nm, τ_0 = 1.6 ± 0.2 μs; λ = 580 nm, τ_0 = 7.0 ± 0.5 μs). A comparison between the electronic absorption and emission spectra of $[Au_3(dmmp)_2]^{3+}$ and $[Au_2(dmpm)_2]^{2+}$ [[dmpm = bis(dimethylphosphino)methane] has been made. The assignment of the lowest electronic excited state in the $(P_2Au)_n$ system has been suggested to be $^3[(d_{\delta^*})(p_\sigma)]$. The excited-state redox potentials of $[Au_3(dmmp)_2]^{3+*}$ and $[Au_2(dmpm)_2]^{2+*}$ have been determined through oxidative quenching experiments with a series of pyridinium acceptors of variable reduction potential.

There has been a growing interest in the study of polynuclear d^{10} metal complexes, which exhibit rich photophysical and photochemical properties.[1,2] Recent examples include $[(M_2(dppm)_3]$,[1a] $[M_2(dba)_3]$[1b] (M = Pd or Pt), $[Au_2(dppm)_2]^{2+}$,[1c,d] $[Au_2(dmb)(CN)_2]$,[1e] and tetrameric complexes of Au^I,[2a] Ag^I,[2b] Cu^I,[2c] and Hg^{II}[2d] [dppm = bis(diphenylphosphino)methane; dba = dibenzylideneacetone; dmb = 1,8-diisocyano-*p*-menthane]. Of particular interest is the nature of the lowest electronic excited states which serves to develop a better understanding of the luminescent properties of d^{10}–d^{10} systems. Herein are described the synthesis, spectroscopic properties, and *X*-ray crystal structure of a novel trinuclear homometallic gold(I) complex, $[Au_3(dmmp)_2]^{3+}$ [dmmp = bis(dimethylphosphinomethyl)methylphosphine]. The present work allows for direct comparison of $[Au_3(dmmp)_2]^{3+}$ and its binuclear analogue $[Au_2(dmpm)_2]^{2+}$ [dmpm = bis(dimethylphosphino)methane] and hence the assignment of the lowest electronic excited states through such systematic variation from dimeric to trimeric gold(I) systems.

Experimental

Bis(dimethylphosphinomethyl)methylphosphine (dmmp) and bis(dimethylphosphino)methane (dmpm) were purchased from Strem Chemicals. Potassium tetrachloroaurate and thiodiglycol (2,2′-thiodiethanol) were obtained from Aldrich Chemical Co., Ltd. Acetonitrile (Mallinkrodt, ChromAR, HPLC grade) was distilled over calcium hydride and potassium permanganate before use. The pyridinium salts were prepared by refluxing the corresponding substituted pyridine with the appropriate alkylating agent such as methyl iodide in acetone–ethanol (1:1 v/v) for 4 h, followed by metathesis in water using ammonium hexafluorophosphate and recrystallization from acetonitrile–diethyl ether.

Crystals of $[Au_3(dmmp)_2][ClO_4]_3$ for *X*-ray crystal structure determination were obtained by recrystallization from hot $HClO_4$ (60 °C).

Synthesis of Gold Complexes.—(*i*) $[Au_2(dmpm)_2][ClO_4]_2$. This compound was prepared according to the published procedure.[1h,3] U.v.-visible (MeCN): λ/nm($\varepsilon_{max.}$/dm^3 mol^{-1} cm^{-1}) 316 (310, sh), 269 (24 700), 239 (5 500), and 213(11 500).

(*ii*) $[Au_3(dmmp)_2][ClO_4]_3$. The salt $K[AuCl_4]$ (2.9 g) was reduced to Au^I by thiodiglycol (4 cm^3) in methanol (100 cm^3). In an argon atmosphere, dmmp (1 g) in methanol (75 cm^3) was added dropwise to give an immediate yellow precipitate, which gradually redissolved to give a pale yellow solution. After stirring for 2 h the reaction mixture was filtered to remove any insoluble material. The filtrate was reduced in volume and to this was added a saturated methanolic solution of $LiClO_4$ (10 cm^3), followed by diethyl ether (60 cm^3). A pale yellow precipitate was obtained. The pure $[Au_3(dmmp)_2][ClO_4]_3$ complex can be obtained as a white solid by washing the pale yellow precipitate with MeCN. White crystalline samples of $[Au_3(dmmp)_2][ClO_4]_3$ were obtained by recrystallization from dilute perchloric acid. Yield: 35% [Found for sample dried under vacuum: C, 13.8; H, 3.1; P, 14.0. Calc. C, 13.1; H, 3.0; P, 14.5%] U.v.-visible (MeCN): λ/nm($\varepsilon_{max.}$/dm^3 mol^{-1} cm^{-1}) 315 (23 360), 242 (9 490), and 218 (11 500).

Physical Measurements and Instrumentation.—U.v.-visible spectra were obtained on a Shimadzu UV-240 spectrophotometer, steady-state emission spectra on a Hitachi 650-60 fluorescence spectrophotometer. Corrected emission spectra were obtained using a Hitachi 650-0178 data processor accessory.

† *Supplementary data available:* see Instructions for Authors, *J. Chem. Soc., Dalton Trans.*, 1990, Issue 1, pp. xix–xxii.

Non. S.I. unit employed: eV = 1.60 × 10^{-19} J.

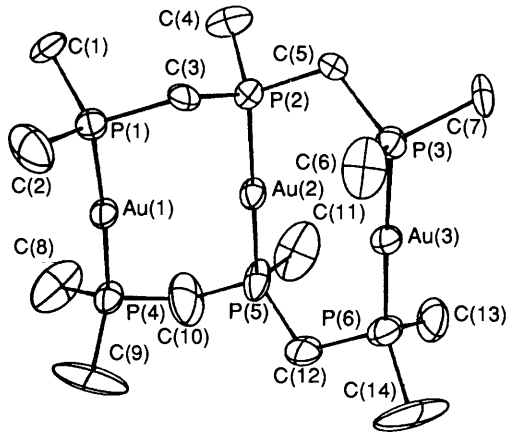

Figure 1. ORTEP drawing of $[Au_3(dmmp)_2]^{3+}$ ion. The thermal ellipsoids are drawn at 35% probability.

Luminescence quenching experiments were monitored by time-resolved (lifetime) emission measurements, and data were treated by a Stern–Volmer fit as described by $\tau_0/\tau = 1 + k_q\tau_0[Q]$, where τ_0 and τ are the respective excited-state lifetimes in the absence and in the presence of quencher Q, k_q is the bimolecular quenching rate constant, and [Q] is the concentration of the quencher. Emission lifetime measurements were performed using a conventional laser system. The excitation source was the 355-nm output (third harmonic) of a Quanta-Ray Q-switched DCR-3 pulsed Nd-YAG laser (10 Hz, G-resonator). Luminescence decay signals were recorded on a Tektronix model 2430 digital oscilloscope, and analyzed using a program for exponential fits. All solutions for quenching studies were prepared under vacuum in a 10-cm^3 roundbottom flask equipped with a sidearm 1-cm fluorescence cuvette and sealed from the atmosphere by a Kontes quick-release Teflon stopper. Solutions were rigorously degassed with no fewer than four freeze–pump–thaw cycles.

Crystal Structure Determination.—Crystal data. $C_{14}H_{38}Au_3Cl_3O_{12}P_6 \cdot 2.5H_2O$, $M_r = 1\,326.59$, monoclinic, space group $P2_1/n$ (alternative $P2_1/c$, no. 14), $a = 12.880(3)$, $b = 14.210(1)$, $c = 21.208(2)$ Å, $\beta = 106.25(1)°$, $U = 3\,727(2)$ Å^3 (by least-squares refinement of diffractometer angles for 25 automatically centred reflections, $\lambda = 0.710\,73$ Å), $D_m = 2.36$ g cm^{-3}, $Z = 4$, $D_c = 2.364$ g cm^{-3}, colourless prisms, crystal dimensions $0.05 \times 0.07 \times 0.14$ mm, μ(Mo-K_α) = 123 cm^{-1}, $F(000) = 2484$.

Data collection and processing. Enraf-Nonius CAD4 diffractometer, ω—2θ mode with ω scan width = 1.0 + 0.34 tanθ, ω speed 1.0—5.5° min^{-1}, graphite-monochromated Mo-K_α radiation; 7 399 reflections measured ($1 < \theta < 25°$; h, k, $\pm l$), 6 272 unique [merging $R = 0.038$ after absorption correction based on azimuthal (ψ) scans of six reflections with $80 < \chi < 90°$ (maximum, minimum transmission factors = 0.999, 0.749)] giving 2 927 with $I > 3\sigma(I)$. Linear and approximate isotropic crystal decay, *ca.* 23%, corrected during data processing.

Structure analysis and refinement. The gold and phosphorus atoms were located by MULTAN 82[4] and all the other non-hydrogen atoms from subsequent Fourier difference syntheses. Hydrogen atoms were omitted in the structure-factor calculation. The refinement was by full-matrix least squares. All non-hydrogen atoms except oxygen were refined anisotropically. The perchlorate ions were badly disordered. Of the three oxygen atoms representing three water molecules one [O(3)] showed an abnormally large isotropic thermal parameter. When an occupancy factor of 0.5 was given to that atom the refinement converged to final $R = 0.047$ and $R' = 0.056$ $\{R = \Sigma\|F_o| - |F_c\|/\Sigma|F_o|$; $R' = [w(|F_o| - |F_c|)^2/\Sigma w|F_o|^2]^{\frac{1}{2}}$, with $w = 4F_o^2/[\sigma^2(F_o^2) + (0.04F_o^2)^2]\}$.

Atomic scattering factors were taken from ref. 5 and all calculations were carried out on a MicroVax II computer using the Enraf-Nonius SDP programs.[6] The final atomic coordinates are given in Table 1, selected bond distances and angles in Table 2.

Additional material available from the Cambridge Crystallographic Data Centre comprises thermal parameters and remaining bond lengths and angles.

Results and Discussion

Reduction of $[AuCl_4]^-$ by thiodiglycol in methanol generated Au^I *in situ*, which rapidly reacted with bridging phosphines to give polynuclear $[Au_2(dmpm)_2]^{2+}$ and $[Au_3(dmmp)_2]^{3+}$ complexes. The structure of $[Au_3(dmmp)_2]^{3+}$ has been established by *X*-ray crystallography.

Figure 1 shows the ORTEP plot of the complex cation. The cation consists of three d^{10} P_2Au^I units held together by the two bridging dmmp ligands, with the perchlorate ions being non-coordinating. The P_2Au units are linear with P–Au–P bond angles ranging from 175.0(2) to 176.2(2)°, consistent with an *sp* hybridization of the Au^I. Similar P–Au–P bond angles were found in $[Au_2(dmpm)_2][ClO_4]_2$ [178.0(3)°][1h] and $[Au_2(dppm)_2][BH_3CN]_2 \cdot 2CH_2Cl_2$ [175.2(2)°].[7] In an analogous trimeric rhodium(I) complex, $[Rh_3(CNCH_3)_6(\mu\text{-dpmp})_2][PF_6]_3$ [dpmp = bis(diphenylphosphinomethyl)phenylphosphine], the P–Rh–P bond angles are also similar [172.4(1)—177.8(1)°].[8] Unlike $[Rh_3(CNCH_3)_6(\mu\text{-dpmp})_2]^{3+}$ where the three Rh atoms approach linearity [RhRhRh 160.2(1)°],[8] the Au–Au–Au bond angle is greatly distorted from rectilinear geometry [136.26(4)°]. Although the small bite distances of the triphosphine ligands could account for this deviation, the value would not be expected to be significantly different from that of $[Rh_3(CNCH_3)_6(\mu\text{-dpmp})_2][PF_6]_3$.[8] Thus the significant deviation of the Au–Au–Au bond angle from 180° probably arises from the high ability of Au atoms to form clusters, with atoms Au(1) and Au(3) bending toward each other as a result of weak attractive interactions. The measured intramolecular Au ··· Au distances of 2.981(1) and 2.962(1) Å are similar to those found in other binuclear gold(I) complexes; for example, the 3.028(2)[1h] in $[Au_2(dmpm)_2][ClO_4]_2$ and 2.982(2) Å[7] in $[Au_2(dppm)_2][BH_3CN]_2 \cdot 2CH_2Cl_2$.

The thermal parameters for the carbon atoms associated with one ligand [C(8)—C(14)] are in general much larger than those for the atoms in the other ligand [C(1)—C(7)]. This might be due to the packing effect. The perchlorate ions are badly disordered. The only hydrogen bonds formed are those between O(1) ··· O(2) [2.73(4) Å] and O(3) ··· O(23) [2.78(6) Å].

Spectroscopy and Photophysical Properties.—The electronic absorption spectra of $[Au_3(dmmp)_2][ClO_4]_3$ and $[Au_2(dmpm)_2][ClO_4]_2$ in acetonitrile are shown in Figure 2. Figure 3 depicts a simplified molecular-orbital diagram which shows the interactions between the molecular orbitals for a series of stacked P_2Au units in D_{2h} symmetry taking the Au ··· Au bond as the *z*-axis. The relative energies of the highest-occupied orbitals in the $D_{\infty h}$ d^{10} P_2Au complex are d_{xz}, $d_{xy} < d_{z^2}$, $d_{yz} < d_{x^2-y^2}$, with the d_{z^2} being mixed with the 6*s* orbital, and the lowest-unoccupied orbital is p_z.[1,9c] The binuclear and trinuclear systems are constructed by interacting two and three P_2Au fragments, respectively. For symmetry reasons, the $d_{\delta^*} \longrightarrow p_\sigma$ transition is expected to be less intense than the $d_{\sigma^*} \longrightarrow p_\sigma$ transition. Although the d_σ–d_{σ^*} splitting is expected to be much greater than d_δ–d_{δ^*}, we suggest that the highest-occupied molecular orbital in $(P_2Au)_2$ and $(P_2Au)_3$ is d_{δ^*} rather than d_{σ^*}.[1d,1h,9d] This is based on the emission properties of this class

Table 1. Fractional co-ordinates for the non-hydrogen atoms in $[Au_3(dmmp)_2][ClO_4]_3 \cdot 2.5H_2O$

Atom	x	y	z	Atom	x	y	z
Au(1)	0.388 54(6)	0.335 68(7)	0.053 67(4)	Cl(3)	0.266 2(6)	0.064 1(5)	0.003 7(3)
Au(2)	0.440 56(6)	0.231 06(7)	0.180 45(3)	C(11)	0.209(2)	0.148(3)	0.212(2)
Au(3)	0.540 66(6)	0.276 28(7)	0.320 66(4)	C(12)	0.276(2)	0.342(2)	0.261(1)
P(1)	0.562 1(4)	0.321 2(5)	0.045 1(2)	C(13)	0.315(2)	0.223(2)	0.375(1)
P(2)	0.604 0(4)	0.191 5(4)	0.164 9(2)	C(14)	0.382(2)	0.418(2)	0.389(2)
P(3)	0.710 1(4)	0.247 6(4)	0.309 5(2)	O(11)	0.079(2)	1.012(2)	0.681(1)
P(4)	0.214 6(4)	0.363 2(5)	0.058 0(2)	O(12)	−0.077(2)	1.019(2)	0.715(1)
P(5)	0.272 7(4)	0.260 3(6)	0.193 7(3)	O(13)	0.031(2)	0.888(3)	0.733(2)
P(6)	0.376 0(5)	0.312 8(5)	0.336 4(3)	O(14)	−0.063(3)	0.931(3)	0.642(2)
C(1)	0.578(2)	0.244(2)	−0.017(1)	O(21)	0.506(2)	0.884(2)	0.306(1)
C(2)	0.624(2)	0.432(2)	0.030(1)	O(22)	0.647(3)	0.987(3)	0.330(2)
C(3)	0.656(1)	0.282(2)	0.123 7(9)	O(23)	0.529(3)	1.007(4)	0.246(2)
C(4)	0.600(2)	0.081(2)	0.119(1)	O(24)	0.466(3)	1.029(4)	0.328(2)
C(5)	0.712(2)	0.174(2)	0.240 5(9)	O(31)	0.294(2)	−0.032(2)	0.010(1)
C(6)	0.784(2)	0.355(2)	0.303(1)	O(32)	0.273(2)	0.097(2)	0.066(1)
C(7)	0.799(2)	0.185(2)	0.376 3(9)	O(33)	0.349(2)	0.110(2)	−0.017(1)
C(8)	0.112(2)	0.323(3)	−0.010(1)	O(34)	0.186(3)	0.083(3)	−0.048(2)
C(9)	0.185(2)	0.483(2)	0.063(2)	O(1)	0.375(2)	0.203(2)	0.552(1)
C(10)	0.174(2)	0.295(4)	0.122(1)	O(2)	0.097(2)	0.873(2)	0.886(1)
Cl(1)	−0.000 4(5)	0.965 1(5)	0.700 0(3)	O(3)	0.902(4)	0.610(4)	0.651(2)
Cl(2)	0.536 3(5)	0.975 3(6)	0.312 8(3)				

Table 2. Selected interatomic distances (Å) and angles (°) with estimated standard deviations (e.s.d.s) in parentheses

Au(1)–P(1)	2.303(5)	Au(1)–P(4)	2.302(6)
Au(2)–P(2)	2.290(6)	Au(2)–P(5)	2.294(7)
Au(3)–P(3)	2.296(5)	Au(3)–P(6)	2.296(7)
Au(1) · · · Au(2)	2.981(1)	Au(2) · · · Au(3)	2.962(1)
av. P–C	1.814 ± 0.037		
P(1)–Au(1)–P(4)	175.0(2)	av. Au–P–C	113.7 ± 1.4
P(2)–Au(2)–P(5)	176.0(3)	av. C–P–C	104.9 ± 3.2
P(3)–Au(3)–P(6)	176.2(2)		

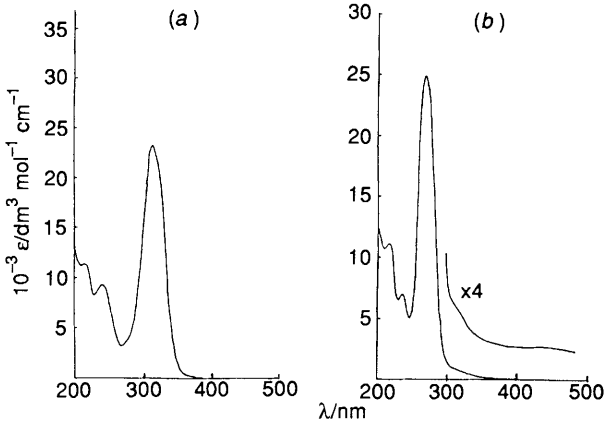

Figure 2. Electronic absorption spectra of (*a*) $[Au_3(dmmp)_2][ClO_4]_3$ and (*b*) $[Au_2(dmpm)_2][ClO_4]_2$ in acetonitrile at room temperature

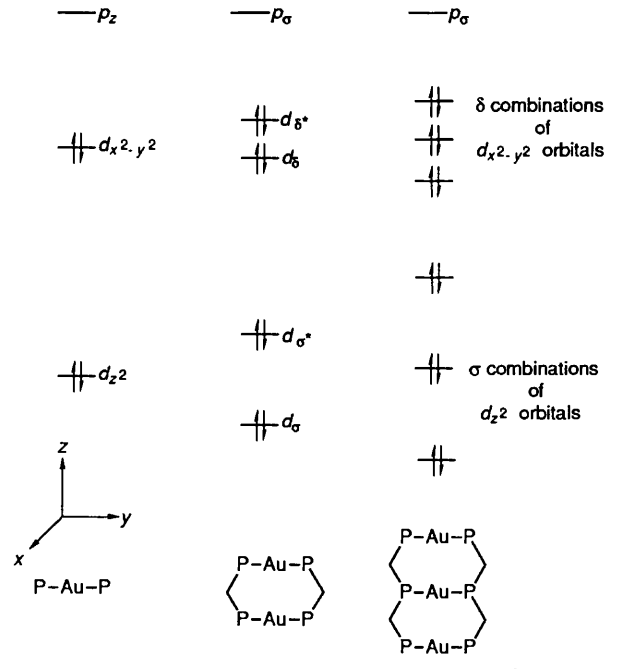

Figure 3. Molecular-orbital interactions for stacking of d^{10} AuP_2 units in D_{2h} symmetry

of compounds as described later in the text. By analogy to the well established pattern in d^8–d^8 species[10] and previous work on related d^{10}–d^{10} systems,[1,9] the intense 315-nm absorption band of $[Au_3(dmmp)_2]^{3+}$ and 269-nm band of $[Au_2(dmpm)_2]^{2+}$ are attributed to the spin-allowed $d_{\sigma^*} \longrightarrow p_\sigma$ transition. The red shift of the transition energy from binuclear to trinuclear species is in accordance with the assignment of the $d_{\sigma^*} \longrightarrow p_\sigma$ transition, since increasing the number of P_2Au units causes narrowing of the $d_{\sigma^*} - p_\sigma$ gap and a rise in energy of the d_{σ^*} orbital. A similar red shift in the $d_{\sigma^*} \longrightarrow p_\sigma$ transition has also been reported in the polynuclear d^8 system.[8]

Excitation of degassed acetonitrile solutions of $[Au_3(dmmp)_2][ClO_4]_3$ and $[Au_2(dmpm)_2][ClO_4]_2$ at 300—370 and 300—350 nm, respectively, at room temperature results in dual phosphorescence (Figure 4). The photophysical data are listed in Table 3. A careful inspection of the emission spectrum of the related $[Au_2(dppm)_2]^{2+}$ system also reveals two emissions at 490 and 570 nm, with the higher-energy emission at 490 nm being more pronounced under non-degassed conditions. For both emissions of the gold complexes the relatively small difference in emission energies upon changing the number of P_2Au units and the very large Stokes shift between the $d_{\sigma^*} \longrightarrow p_\sigma$ transition energies and the emission energies suggest that the lowest emitting electronic states are unlikely to be derived from the $(d_{\sigma^*})^1(p_\sigma)^1$ triplet, as suggested in previous

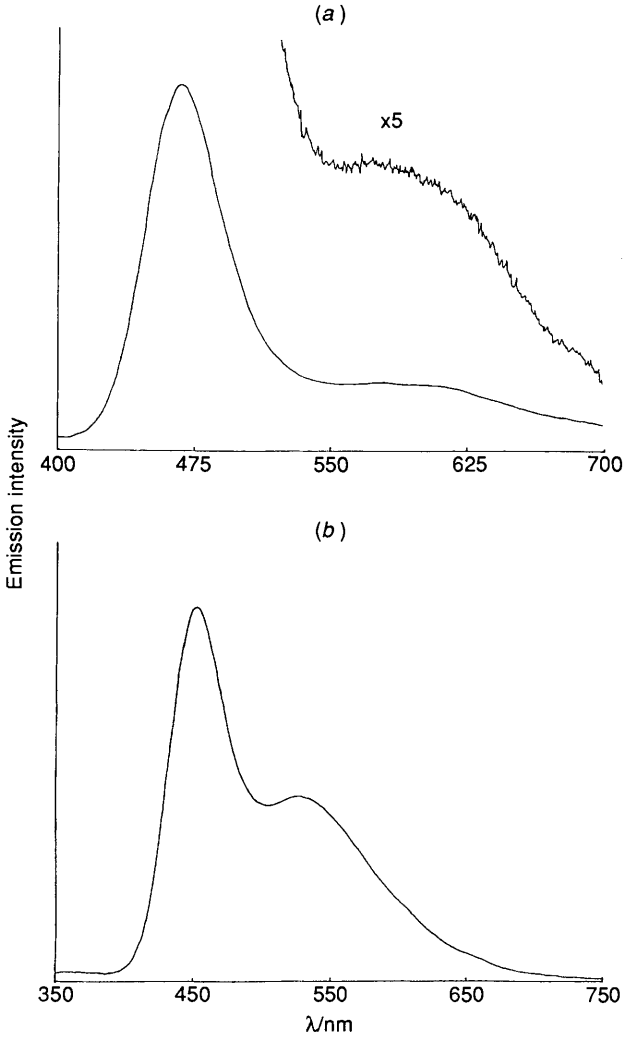

Figure 4. Emission spectrum of (*a*) $[Au_3(dmmp)_2][ClO_4]_3$ (*b*) $[Au_2(dmpm)_2][ClO_4]_2$ in degassed acetonitrile at 25 °C

Table 3. Photophysical data for $[Au_3(dmmp)_2][ClO_4]_3$ and $[Au_2(dmpm)_2][ClO_4]_2$ in degassed acetonitrile at room temperature

Complex	$\lambda_{abs.}$/nm ($\varepsilon_{max.}$/dm^3 mol^{-1} cm^{-1})	$\lambda_{em.}$/nm	τ_o/μs
$[Au_3(dmmp)_2]$-$[ClO_4]_3$	218 (11 500), 242 (9 490), 315 (23 360)	467 580	1.6 ± 0.2 7.0 ± 0.5
$[Au_2(dmpm)_2]$-$[ClO_4]_2$	213 (11 500), 239 (5 500), 269 (24 700), 316 (310,sh)*	455 555	1.2 ± 0.2 2.8 ± 0.2

* From ref. 3.

work.[1d,h,9d] We suggest that the high-energy emission comes from the intraligand spin-forbidden transition of the phosphine ligands since intraligand emissions of PPh_3 complexes of Hg^{2+} and Cu^+ are found to occur at similar energies.[2d,11] The low-energy emission of the polyhomometallic gold(I) system probably is $(d_{\delta^*})^1(p_\sigma)^1$ in origin. With this assumption, we assign the emission bands at 455 nm of $[Au_2(dmpm)_2]^{2+}$ and 467 nm of $[Au_3(dmmp)_2]^{3+}$ to intraligand spin-forbidden transitions of the phosphine ligands. The bands at 555 and 580 nm of both $[Au_2(dmpm)_2]^{2+}$ and $[Au_3(dmmp)_2]^{3+}$ are assigned as phosphorescence derived from the $(d_{\delta^*})^1(p_\sigma)^1$ excited triplet. The relatively small change in energy of this emission from $[Au_2(dmpm)_2]^{2+}$ to $[Au_2(dppm)_2]^{2+}$ (*ca.* 570 nm) is also in accord with the formulation that the electronic transition involved is metal-localized in nature.

Oxidative Quenching with Pyridinium Acceptors.—The phosphorescence of $[Au_3(dmmp)_2]^{3+*}$ and $[Au_2(dmpm)_2]^{2+*}$ is found to be quenched by a number of electron acceptors. Excitation of the gold(I) complexes in the presence of methyl viologen (1,1′-dimethyl-4,4′-bipyridinium dichloride, $dmbipy^{2+}$ $2Cl^-$) in degassed acetonitrile at 355 nm results in transient absorptions peaking at 395 and 600 nm, typical of the $dmbipy^+$ cation radical.[12] The nature of the reaction is suggested to be as in equations (1) and (2). In the wavelength region 350—700 nm

$$[Au_2(dmpm)_2]^{2+*} + dmbipy^{2+} \longrightarrow [Au_2(dmpm)_2]^{3+} + dmbipy^+ \quad (1)$$

$$[Au_3(dmmp)_2]^{3+*} + dmbipy^{2+} \longrightarrow [Au_3(dmmp)_2]^{4+} + dmbipy^+ \quad (2)$$

no absorption of $[Au_3(dmmp)_2]^{4+}$ or $[Au_2(dmpm)_2]^{3+}$ is observed. This may be due to the strong absorption of $dmbipy^+$ superimposed on the much weaker absorption of the oxidized gold complexes.

The phosphorescent states of $[Au_3(dmmp)_2]^{3+*}$ and $[Au_2(dmpm)_2]^{2+*}$ in acetonitrile also undergo facile electron-transfer quenching with pyridinium acceptors. In order further to understand the electron-transfer reactivity of the $^3[(d_{\delta^*})^1(p_\sigma)^1]$ excited state of the gold(I) complexes, a study of electron-transfer quenching by a series of pyridinium acceptors of variable reduction potential was undertaken.[13] The quenching rate constants are summarized in Tables 4 and 5. Excited-state redox potentials of $E[Au_3(dmmp)_2{}^{4+/3+*}] = -1.6(1)$V *vs.* s.c.e. [$\lambda = 0.90(10)$eV, $RT\ln K\kappa\nu = 0.56(10)$V *vs.* s.c.e.] and $E[Au_2(dmpm)_2{}^{3+/2+*}] = -1.7(1)$V *vs.* s.c.e. [$\lambda = 0.95(10)$eV, $RT\ln K\kappa\nu = 0.57(10)$V *vs.* s.c.e.] have been obtained by three-parameter, non-linear least-squares fits to equation (3)[14] where k_q' is the rate constant corrected for

$$\left(\frac{RT}{F}\right)\ln k_q' = \left(\frac{RT}{F}\right)\ln K\kappa\nu - \frac{\lambda}{4}\left(1 + \frac{\Delta G}{\lambda}\right)^2 \quad (3)$$

diffusional effects, $K = k_d/k_{-d}$ which is approximately 1—2 dm^3 mol^{-1}, k_d is the diffusion-limited rate constant in acetonitrile which is taken to be 1.0×10^{10} dm^3 mol^{-1} s^{-1}, κ is the transmission coefficient, ν is the nuclear frequency, λ is the reorganization energy for electron transfer, and ΔG, the standard free-energy change of the reaction, is given by equation (4) for oxidative quenching, where ω_r and ω_p are work terms for

$$\Delta G = E^\circ[Au^{(n+1)+/n+*}] - E^\circ(Q^{+/0}) + \omega_p - \omega_r \quad (4)$$

bringing reactants or products to the mean separation for reaction. The work term associated with the gold(I) complex and a pyridinium acceptor is 0.01—0.03 eV. This contribution is neglected in the analysis of the electron-transfer rate data. Figures 5 and 6 show the theoretical fits. The close agreement between the theoretical curve with the experimental data is in accordance with the fact that the photoreactions are outer-sphere electron transfer in nature. The stronger reducing power of $[Au_2(dmpm)_2]^{2+*}$ than $[Au_3(dmmp)_2]^{3+*}$ is understandable on the grounds that the latter with a charge of 3+ is more difficult to be oxidized. Interestingly, the estimated λ values for both the $[Au_3(dmmp)_2]^{3+}$ and $[Au_2(dmpm)_2]^{2+}$ systems are similar, and are comparable to the value of *ca.* 1.06 eV found for the reaction between the $^3(d_{\sigma^*}p_\sigma)$ state of Ir_2 and pyridinium acceptors in $[Ir_2(\mu\text{-dmpz})_2(CO)_2\{Ph_2PO(CH_2)_2A\}_2]$ (dmpz = 3,5-dimethylpyrazolyl, A = *N*-alkylpyridinium acceptor).[15]

Table 4. Rate constants for the quenching of $[Au_2(dmpm)_2]^{2+*}$ by pyridinium acceptors in acetonitrile (0.1 mol dm^{-3} $NBu^n_4PF_6$) at 25 °C

Quencher[a]	$E(A^{+/0})^b$/V *vs.* s.c.e.	k_q/dm^3 mol^{-1} s^{-1}	$k_q'^c$/dm^3 mol^{-1} s^{-1}	ln k_q'
4-Cyano-*N*-methylpyridinium	−0.67	5.15×10^9	6.94×10^9	22.66
4-Methoxycarbonyl-*N*-methylpyridinium	−0.78	2.46×10^9	2.81×10^9	21.76
4-Aminoformyl-*N*-ethylpyridinium	−0.93	2.28×10^9	2.57×10^9	21.67
3-Aminoformyl-*N*-methylpyridinium	−1.14	4.60×10^8	4.71×10^8	19.97
N-Ethylpyridinium	−1.36	5.78×10^7	5.79×10^7	17.88
4-Methyl-*N*-methylpyridinium	−1.49	5.66×10^7	5.68×10^7	17.85
2,6-Dimethyl-*N*-methylpyridinium	−1.52	4.77×10^6	4.77×10^6	15.38

[a] All the compounds are hexafluorophosphate salts. [b] Ref. 13. [c] See ref. 14.

Table 5. Rate constants for the quenching of $[Au_3(dmmp)_2]^{3+*}$ by pyridinium acceptors in acetonitrile (0.1 mol dm^{-3} $NBu^n_4PF_6$) at 25 °C

Quencher[a]	$E(A^{+/0})^b$/V *vs.* s.c.e.	k_q/dm^3 mol^{-1} s^{-1}	$k_q'^c$/dm^3 mol^{-1} s^{-1}	ln k_q'
4-Cyano-*N*-methylpyridinium	−0.67	3.87×10^9	6.31×10^9	22.57
4-Methoxycarbonyl-*N*-methylpyridinium	−0.78	1.88×10^9	2.32×10^9	21.56
4-Aminoformyl-*N*-ethylpyridinium	−0.93	1.33×10^9	1.53×10^9	21.15
3-Aminoformyl-*N*-methylpyridinium	−1.14	2.96×10^8	3.05×10^8	19.54
N-Ethylpyridinium	−1.36	2.32×10^7	2.32×10^7	16.96
4-Methyl-*N*-methylpyridinium	−1.49	1.23×10^7	1.24×10^7	16.33
2,6-Dimethyl-*N*-methylpyridinium	−1.52	2.56×10^6	2.56×10^6	14.76

[a] All the compounds are hexafluorophosphate salts. [b] Ref. 13. [c] See ref. 14.

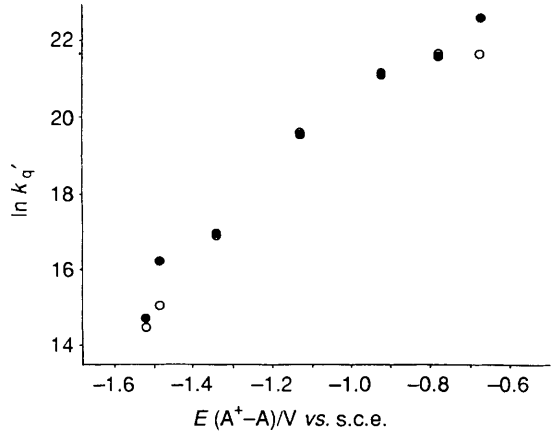

Figure 5. Plot of ln k_q' *versus* $E(A^{+/0})$ for the electron-transfer quenching of $[Au_3(dmmp)_2]^{3+*}$ by pyridinium acceptors in degassed acetonitrile: (●) experimental; (○) calculated

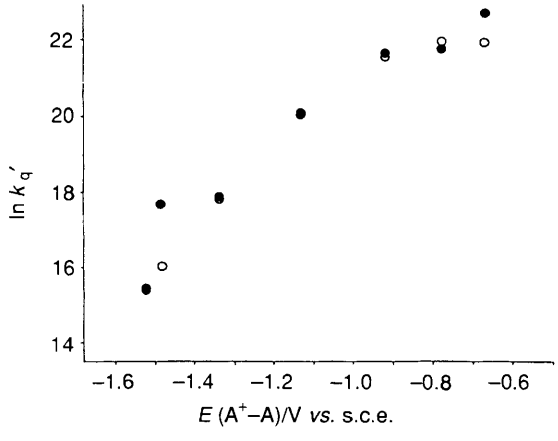

Figure 6. Plot of ln k_q' *versus* $E(A^{+/0})$ for the electron-transfer quenching of $[Au_2(dmpm)_2]^{2+*}$ by pyridinium acceptors in degassed acetonitrile: (●) experimental; (○) calculated

Conclusion

There are few polynuclear metal complexes with long-lived excited states in fluid solutions.[16] The present work demonstrates that such species can easily be assembled by utilizing Au^I and polydentate phosphine ligands. The co-ordinatively unsaturated nature and the strong reducing power of the triplet excited states of polymetallic gold(I) phosphine species should make this class of compounds a good model system for studies of oxidative-addition reactions involving d^{10} metal species.

Acknowledgements

V.W-W.Y. acknowledges financial support from the City Polytechnic of Hong Kong (Indicated Grant No. 7015). Financial support from the University of Hong Kong and the Croucher Foundation is also gratefully acknowledged. We thank Professor H. B. Gray for sending us a preprint of his work on $[M_2(dppm)_3]$ prior to publication. T. M. McCleskey is thanked for his assistance in steady-state emission experiments at Caltech.

References

1 (*a*) P. D. Harvey and H. B. Gray, *J. Am. Chem. Soc.*, 1988, **110**, 2145; (*b*) P. D. Harvey, F. Adar, and H. B. Gray, *ibid.*, 1989, **111**, 1312; (*c*) C. M. Che, H. L. Kwong, V. W. W. Yam, and K. C. Cho, *J. Chem. Soc., Chem. Commun.*, 1989, 885; C. M. Che, H. L. Kwong, V. W. W. Yam, and C. K. Poon, *J. Chem. Soc., Dalton Trans.*, 1990, 3215; (*d*) C. King, J. C. Wang, N. I. Md. Khan, and J. P. Fackler, jun., *Inorg Chem.*, 1989, **28**, 2145; (*e*) C. M. Che, W. T. Wong, T. F. Lai, and H. L. Kwong, *J. Chem. Soc., Chem. Commun.*, 1989, 243; (*f*) J. V. Caspar, *J. Am. Chem. Soc.*, 1985, **107**, 6718; (*g*) J. P. Fackler, jun., and J. D. Basil, *ACS Symp. Ser.*, 1983, **211**, 201; (*h*) H. R. C. Jaw, M. M. Savas, R. D. Rogers, and W. R. Mason, *Inorg. Chem.*, 1989, **28**, 1028; (*i*) N. I. Md. Khan, J. P. Fackler, jun., C. King, J. C. Wang, and S. Wang, *Inorg. Chem.*, 1988, **27**, 1672.

2 (*a*) A. Vogler and H. Kunkely, *Chem. Phys. Lett.*, 1988, **150**, 135; (*b*) A. Vogler and H. Kunkely, *ibid.*, 1989, **158**, 74; (*c*) K. R. Kyle, J. DiBenedetto, and P. C. Ford, *J. Chem. Soc., Chem. Commun.*, 1989, 714; (*d*) H. Kunkely and A. Vogler, *Chem. Phys. Lett.*, 1989, **164**, 621.

3 W. Ludwig and W. Meyer, *Helv. Chim. Acta*, 1982, **65**, 934.

4 P. Main, S. J. Fiske, S.E. Hull, I. Lessinger, G. Germain, J. P.

Declereq, and M. M. Woolfson, 'MULTAN 82. A System of Computer Programmes for the Automatic Solution of Crystal Structures,' Universities of York and Louvain, 1982.
5 'International Tables for *X*-Ray Crystallography,' Kynoch Press, Birmingham, 1974, vol. 4, pp. 99—149.
6 'Enraf-Nonius Structure Determination Package,' SDP, Enraf-Nonius, Delft, 1985.
7 N. I. Md. Khan, C. King, D. D. Heinrich, J. P. Fackler, jun., and L. C. Porter, *Inorg. Chem.*, 1989, **28**, 2150.
8 A. L. Balch, L. A. Fossett, J. K. Nagle, and M. M. Olmstead, *J. Am. Chem. Soc.*, 1988, **110**, 6732.
9 (*a*) W. R. Mason, *J. Am. Chem. Soc.*, 1976, **98**, 5182; (*b*) S. K. Chastain and W. R. Mason, *Inorg. Chem.*, 1982, **21**, 3717; (*c*) M. M. Savas and W. R. Mason, *ibid.*, 1987, **26**, 301; (*d*) H. R. C. Jaw, M. M. Savas, and W. R. Mason, *ibid.*, 1989, **28**, 4366.
10 D. M. Roundhill, H. B. Gray, and C. M. Che, *Acc. Chem. Res.*, 1989, **22**, 55; S. F. Rice, S. J. Milder, H. B. Gray, R. A. Goldbeck, and D. S. Kliger, *Coord. Chem. Rev.*, 1982, **43**, 349.
11 D. P. Segers, M. K. DeArmond, P. A. Grutsch, and C. Kutal, *Inorg. Chem.*, 1984, **23**, 2874.
12 E. M. Kosower and J. L. Cotter, *J. Am. Chem. Soc.*, 1964, **86**, 5524.
13 J. L. Marshall, S. R. Stobart, and H. B. Gray, *J. Am. Chem. Soc.*, 1984, **106**, 3027.
14 C. R. Bock, J. A. Connor, A. R. Gutierrez, T. J. Meyer, D. G. Whitten, B. P. Sullivan, and J. K. Nagle, *J. Am. Chem. Soc.*, 1979, **101**, 4815.
15 L. S. Fox, M. Kozik, J. R. Winkler, and H. B. Gray, *Science*, 1990, **247**, 1069.
16 A. W. Maverick and H. B. Gray, *J. Am. Chem. Soc.*, 1981, **103**, 1298.

Received 10*th May* 1990; *Paper* 0/02068K